Multicolor linear polarimetry of Betelgeuse and Antares

Tinbergen, J.; Greenberg, J.M.; Jager, C. de

Astron. Astrophys. 95, 215–220 (1981)

ASTRONOMY AND ASTROPHYSICS

Multicolor Linear Polarimetry of Betelgeuse and Antares*

J. Tinbergen[1], J. M. Greenberg[2], and C. de Jager[3]

1 Sterrewacht, Postbus 9513, 2300 RA Leiden, The Netherlands
2 Laboratory Astrophysics, Huygens Laboratory, Postbus 9504, 2300 RA Leiden, The Netherlands
3 The Astronomical Institute, Beneluxlaan 21, 3527 HS Utrecht, The Netherlands

SUMMARY. Multicolor linear polarimetry of α Ori and Sco confirms in a qualitative way the ideas about large-scale moving elements in these stellar atmospheres, as suggested by Schwarzschild (1975).

For one well-observed scattering element, we deduce from the observations a relation between the degree of ionization and the fraction of silicon condensed in grains.

Sizable residuals remain at short and long wavelengths. Time variations of the short-wavelength residuals suggest time variations in the dust formed in the stellar atmospheres.

KEY WORDS: Convection - stellar atmospheres - polarization - α Ori - α Sco

1. INTRODUCTION

While engaged primarily on other polarimetric programmes, one of us (J.T.) took the opportunity to observe Betelgeuse (α Ori, M2 Iab) and Antares (α Sco, M1.5 Iab) repeatedly in 7 or 8 bands within the interval 400 to 850 nm. The intention was to learn something more about the mechanism of the well-known variable polarization of these stars, without having well-defined ideas about what to look for.

After the observations were made, it seemed that they might be a good test of the ideas, outlined by Stothers and Leung (1971) and by Schwarzschild (1975), concerning the scale of photospheric convection in such stars.

An analysis of the data for α Ori yields support to the hypothesis that during the greater part of the observing period the stellar photosphere was dominated by one or at most a few large moving elements.

2. INSTRUMENT AND OBSERVATIONS

The Leiden polarimeter has three simultaneous channels, each with a choice of filters, and uses an achromatic modulator (Tinbergen, 1973); it allows polarimetry with an accuracy of better than 10^{-4} in degree of polarization, given sufficient photons and a certain minimum integration time to overcome residual scintillation noise. The filter passbands used in the present programme are shown in Fig. 1. Three telescopes were used; all were Cassegrain systems. Two of them showed negligible instrumental polarization, while for the third (Leiden Southern Station, at that time at Hartebeespoortdam) it was both strong and wavelength-dependent, but could be determined and has been removed from the data. The remainder of the reduction consisted of corrections for the slight wavelength-dependence of the modulation efficiency and the zero of polarization angle (respectively 8% and 3%4 total variation over the wavelength range quoted). Standard polarized stars were used to determine the rotation of the instrumental coordinate system. All results are expressed in the usual astronomical system, with the +Q axis (θ = 0) corresponding to the equatorial N-S direction and degree of polarization expressed as a fraction. Tables 1 and 2 give the results; where convenient, averages over periods of about 1 week were formed to reduce noise. The observations are also displayed in Figs. 2 and 3.

We note the following points:

a. Variations in polarization are present and they are not of a very simple character (this is not new, of course).
b. The variations are strongest in the blue part of the spectrum, noticeably weaker in the near infrared (also observed previously).
c. Polarizations in bands 3,4,5 and 6 generally fall on a straight line in the Stokes vector plots; the other bands often (but not always) deviate significantly.
d. The lines mentioned in c. do not have constant orientation.
e. The lengths of the polarization difference vectors between adjacent spectral bands do not always vary in the same way with time; p(3) minus p(4) in Betelgeuse - while remaining on the straight line - is such a case.

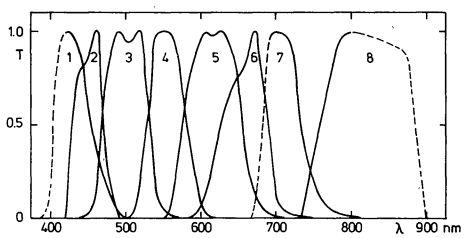

Fig. 1. Passbands of the Leiden polarimeter. Solid curves denote filter transmissions, while dashed curves are approximate positions of cut-offs by the photomultipliers or by optical components permanently in the beam.

* Based in part on observations at the European Observatory, La Silla, Chile.

Send offprint requests to: J. Tinbergen

Table 1. Degree of polarization of Betelgeuse, expressed as Q and U values, in units of 10^{-4} (0.01%). Positive Q is equatorial N-S.

Passband / filter § / period / λ_{eff}	1 BG 12 425	2 K 2 450	3 K 3 500	4 K 4 550	5 K 5 620	6 K 6 660	7 K 7 710	8 RG 780 825 nm	n	Location	Telescope diameter (cm)
a: 01.12.1973		-3;-27	-6;-23	-1;-19	-1;-24	+1;-17	-6;-24	-3;-27	1	Leiden	30
b: 01.02-06.02 1974		-19;-67 ± 1	-17;-72 ± 2	-9;-59 ± 1	0;-51 ± 1	-3;-50 ± 2	-10;-53 ± 2	-11;-49 ± 1	6	La Silla	50
c: 19.02-24.02 1974		-34;-90 ± 2	-30;-98 ± 2	-21;-81 ± 1	-10;-63 ± 1	-9;-60 ± 2	-14;-64 ± 1	-16;-58 ± 2	6	La Silla	50
d: 27.02-06.03 1974		-39;-95 ± 1	-38;-100 ± 2	-29;-88 ± 1	-12;-71 ± 1	-8;-66 ± 1	-19;-68 ± 1	-18;-63 ± 1	8	La Silla	50
e: 07.03-14.03 1974		-48;-98 ± 3	-47;-107 ± 2	-37;-88 ± 1	-18;-74 ± 1	-16;-70 ± 1	-25;-71 ± 1	-21;-62 ± 1	6	La Silla	50
f: 23.08-26.08 1974	-39;-90 ± 7	-19;-80 ± 2	-17;-71 ± 6	-9;-66 ± 1	-4;-52 ± 1	+2;-46 ± 1	+11;-46 ± 1	+16;-37 ± 1	3	HBP*	93
g: 04.02-08.02 1975	+54;-72 ± 2	+52;-62 ± 3	+48;-59 ± 2	+46;-50 ± 2	+35;-41 ± 1	+30;-37 ± 3	+31;-46 ± 1	+21;-41 ± 3	3	Leiden	30

*HBP: Leiden Southern Station, at that time at Hartebeestpoortdam, S. Africa.

§Balzers K-series and Schott glass filters.

Table 2. Degree of polarization of Antares, expressed as Q and U values, in units of 10^{-4} (0.01%). Positive Q is equatorial N-S.

passband / filter § / period / λ_{eff}	1 BG 12 425	2 K 2 450	3 K 3 500	4 K 4 550	5 K 5 620	6 K 6 660	7 K 7 710	8 RG 780 825 nm	n	Location	Telescope diameter (cm)
A: 03.02-06.02 1974		0;+25 ± 2	-7;+21 ± 1	-8;+31 ± 1	-7;+38 ± 2	-5;+33 ± 4	-15;+34 ± 1	-15;+33 ± 1	5	La Silla	50
B: 18.02-24.02 1974		+1;+28 ± 1	-4;+29 ± 1	-6;+35 ± 1	-5;+40 ± 1	-6;+41 ± 1	-15;+38 ± 1	-15;+35 ± 2	7	La Silla	50
C: 27.02-06.03 1974		0;+26 ± 2	-3;+24 ± 1	-5;+33 ± 1	-5;+35 ± 1	-7;+36 ± 1	-16;+33 ± 1	-17;+33 ± 2	8	La Silla	50
D: 07.03-14.03 1974		+4;+25 ± 1	-4;+22 ± 3	-5;+35 ± 2	-9;+37 ± 2	-7;+33 ± 2	-15;+32 ± 1	-15;+32 ± 2	5	La Silla	50
E: 10.07.1974		-7;+18	-7;+31	-8;+31	-13;+37	-14;+41			1	HBP*	93
F: 18.07.1974	-2;+32	-6;+31	-6;+33	-8;+37	-12;+41	-12;+43	-15;+46	-14;+46	1	HBP*	93
G: 25.07.1974	-4;+33	-2;+35	-2;+43	-4;+43	-7;+46	-11;+48	-12;+47	-14;+47	1	HBP*	93
H: 09.08.1974	+1;+38	+1;+37	+1;+46	-1;+47	-10;+52	-10;+53	-11;+49	-11;+48	1	HBP*	93
I: 23.08.1974	+7;+42	+6;+37	+7;+45	+2;+48	-4;+52	-5;+50	-9;+50	-11;+47	1	HBP*	93

*HBP: Leiden Southern Station, at that time at Hartebeestpoortdam, S. Africa.

§Balzers K-series and Schott glass filters.

3. THE 'INTERSTELLAR' COMPONENT

Points c. and d. above tempt one to try a separation into an interstellar component (identified as the intersection of the straight lines mentioned; constant in time, with λ_{max} = 550 nm, and therefore roughly constant over bands 3 to 6) and an intrinsic component which is strongest in the blue and has an orientation which does vary with time but only weakly with wavelength. For the Betelgeuse observations, this is a possible construction, with $(Q,U)_{interst.}$, λ_{max} = = (+18;-20) x 10^{-4} (Fig. 4). However, it does not solve all it set out to: although it does improve the colinearity of the February/March 1974 data (periods b-e), it does not make it complete; secondly, it hardly affects the data of February 1975 (period g); finally, there is evidence in Fig. 4 that the 'interstellar' component is not strictly constant over the years; so

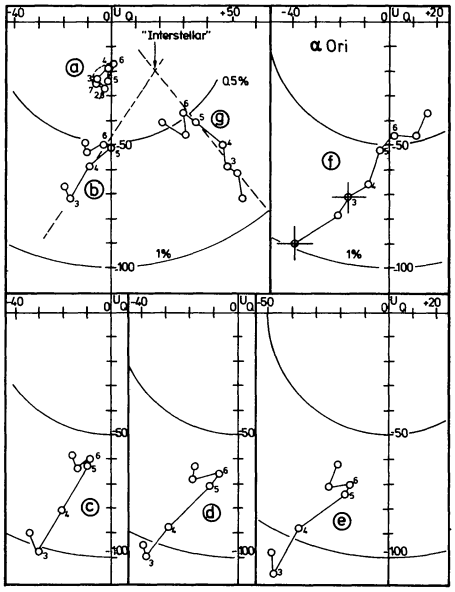

Fig. 2. Polarization of Betelgeuse for the different observing periods, designated a - g, as in Table 1. Passbands are numbered. The radius of the small circles is approximately 1σ.

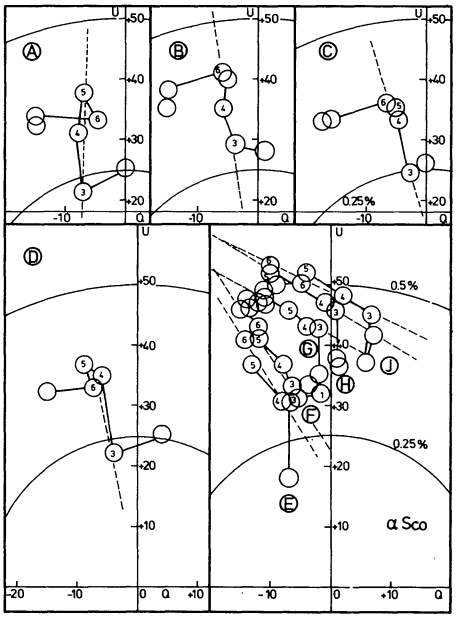

Fig. 3. Polarization of Antares for the various observing periods, designated A - I, as in Table 2. Passbands are numbered. The radius of the small circles is approximately 1σ.

perhaps it should - partly - be identified with a slowly varying circumstellar component. For Antares, the 'interstellar' component identified from the more variable July/August 1974 data (periods E-I) is approximately (-20;+55) x 10^{-4}, but this is inconsistent with the data for February/March 1974 (periods A-D): though the results for bands 3 to 6 lie on a straight line, this line misses the 'interstellar' point by about 10^{-3}

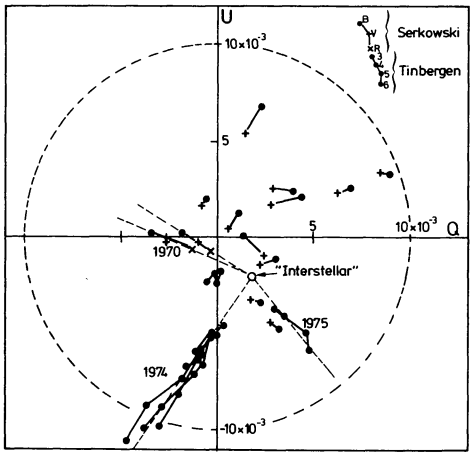

Fig. 4. Determination of the 'interstellar' component for α Ori multicolor observations made by K. Serkowski and J. Tinbergen. $(Q;U)_{interst.}$ = (18;-20) in units of 10^{-4}.

in degree of polarization, i.e. by an estimated 3 to 5σ. In the rest of the paper we shall mainly discuss α Ori; α Sco behaves in a generally similar way and, where possible, we shall include it in the analysis. In particular it is possible to fit a λ^{-4} law at constant angle through the observed points for passbands 3 to 6, without worrying about the time-varying 'interstellar' component.

4. THE 'INTRINSIC' COMPONENT FOR α ORI

a) Wavelength dependence

For α Ori, the interstellar component can be identified fairly well, and the same therefore holds for the ('intrinsic') stellar component. A plot of the intrinsic degree of polarization p against wavelength (Fig. 5) shows monotonic decrease of p with λ, at least for passbands 3 through 6. This fact, taken with the straight lines in the Stokes vector plots (Fig. 2), suggests that one single physical process is responsible for the polarization in this wavelength range. Since $p \sim \lambda^{-4}$ fits well in this wavelength range, it seems reasonable to attribute this polarization to Rayleigh scattering in an asymmetric, or asymmetrically illuminated, gas or dust cloud in the atmosphere or in the vicinity of the star. Since, in addition, it seems that for most dates $\lim p(\lambda \to \infty) \neq 0$, we have to add a constant contribution, possibly due to scattering by free electrons in probably the same cloud, since the polarization angle is the same.

We represent the total intrinsic polarization by:

$$p \sim n_d \sigma_d + n_H \sigma_H + n_e \sigma_e \qquad (1)$$

where n_d, σ_d, n_H, σ_H, and n_e, σ_e, are the number densities and scattering cross-sections of the dust grains, the hydrogen atoms, and the electrons respectively. The scattering contribution by helium or other atoms and molecules is negligible. The dust grains are likely to be small silicate particles, as inferred from evidence for formation in other cool stars (see Salpeter 1977 for a recent review) and as indicated by an apparent 10μ excess in α Ori (Merrill and Stein, 1976; Merrill 1977).

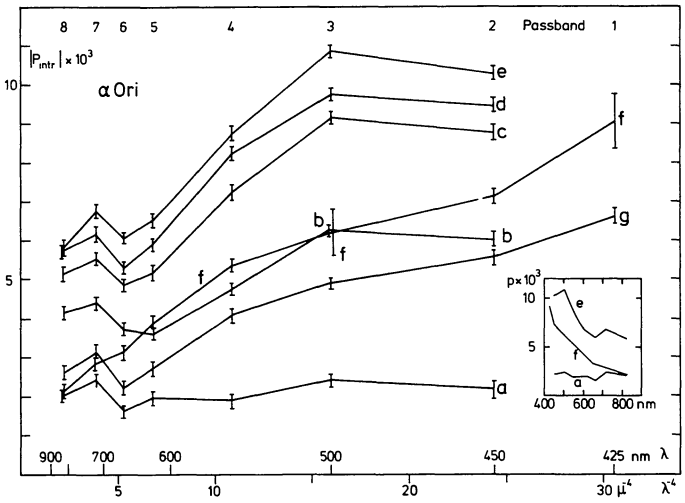

Fig. 5. Intrinsic polarization of α Ori for the seven observing periods, designated by letters a - g as in Table 1. The p-values are plotted against λ and against λ^{-4}. As a rule the observations in the passbands (3), 4,5,6 fall on a straight line in the λ^{-4} plot. The gradient of the line gives the n_H/n_e value, while the p-value for $\lambda^{-4} = 0$ indicates the wavelength independent contribution, i.e. the polarization component presumably due to scattering at free electrons.

The cross-section of each of the atmospheric scattering constituents is given in cm^2 by:

$$\sigma_d = \frac{8\pi}{3}\left[a_d^2\left(\frac{2\pi a_d}{\lambda}\right)^4\left|\frac{\varepsilon-1}{\varepsilon+2}\right|^2\right] \qquad (2a)$$

$$\sigma_H = \sigma_e \cdot \left(\frac{\lambda_o}{\lambda}\right)^4 \qquad (2b)$$

$$\sigma_e = \frac{8\pi}{3}\left(\frac{e^2}{mc^2}\right)^2 \qquad (2c)$$

where: in Eq. 2a the dust grains are approximated by small ($2\pi a_d/\lambda \lesssim 0.5$) spherical particles of radius a_d and dielectric coefficient ε; in Eq. 2b the H atoms are approximated as bound electrons with resonance frequency $\nu_o = c/\lambda_o$, λ_o = 102.6 nm (cf. Unsöld 1955, p. 177 ff.); and Eq. 2c represents the Thomson scattering cross-section for free electrons.

The sum of the polarizing components is then:

$$P_{total} \sim n_e \sigma_e \left\{1 + \frac{n_H}{n_e}\left(\frac{0.1026}{\lambda}\right)^4 + \frac{n_d}{n_e}\left(\frac{a_d}{0.05}\right)^6\left(\frac{777}{\lambda}\right)^4\right\} \qquad (3)$$

where a_d and λ are measured in μm. We have assumed a constant index of refraction, m = 1.6, for the dust grains over the wavelength range observed.

We may make an upper estimate of the number of dust grains by assuming that all of the heavy elements by cosmic abundance are condensed in the form of solid particles. As an illustration, consider olivine (Mg_2SiO_4) to be the characteristic silicate. Then, adopting a cosmic abundance for silicon of 0.32×10^{-4} relative to hydrogen (e.g. Greenberg 1978 for a recent dust review), we obtain:

$$\frac{n_d}{n_H} = \frac{n_d}{n_{si}} \cdot \frac{n_{si}}{n_H + n_e} \cdot \frac{n_H + n_e}{n_H}$$

$$= 1.35 \times 10^{-7}\left(\frac{0.05}{a_d}\right)^3 \cdot 0.32 \times 10^{-4} A \cdot \frac{n_H + n_e}{n_H}$$

$$= 4.3 \times 10^{-12}\left(\frac{0.05}{a_d}\right)^3 \cdot A \cdot \frac{n_H + n_e}{n_H} \qquad (4)$$

where A denotes the fraction of the 'cosmic-abundance-silicon' actually condensed in the dust grains. We have used 3.3 for the density of olivine, $n_H + n_e$ for the total number of hydrogen atoms and ions, and have assumed that all the dust grains are characterized by the mean size a_d.

Substituting Eq. 4 into Eq. 3 we obtain:

$$P_{total} \sim n_e \sigma_e \left\{1 + \frac{n_H}{n_e}\left(\frac{0.1026}{\lambda}\right)^4 \times \left(1 + 1.4 \times 10^4 \cdot A \cdot \frac{n_H + n_e}{n_H} \cdot \left(\frac{a_d}{0.05}\right)^3\right)\right\} \qquad (5)$$

Since we do not know the scattering configuration, the absolute value of the polarization does not provide us with the possibility of a complete interpretation of Eq. (5). However, the relative strengths of the λ^{-4} and the λ^0 components do put restrictions on the scattering medium, if we assume that the two components arise in the same volume of space (a reasonable assumption, given the nearly equal polarization angles).

In Table 3 we have tabulated the two components and their ratio (P_T = Thompson polarization, P_{R15} = Rayleigh polarization at λ = 0.508 μm, i.e. $\lambda^{-4} = 15(\mu m)^{-4}$). Disregarding period a (Fig. 2 shows why), the ratio P_{R15}/P_T varies around 3. Taking this as an example, we

Table 3. Thomson and Rayleigh polarizations for α Ori.

Period	$\lvert P_T\rvert \times 10^4$	$\lvert P_R\rvert \times 10^4$ at $\lambda^{-4} = 15(\mu m)^{-4}$	$\lvert P_{R15}\rvert / \lvert P_T\rvert$
(a)	(15)	(10)	(0.7)
b	15	45	3
c	25	60	2.4
d	30	65	2.2
e	35	70	2
f	15	50	3.7
g	10	40	4

Table 4. α Ori. Representative values of condensed fraction A and $k = n_e/n_H$.

A	x	$k = n_e/n_H$	a_d (μm)
0	0	6×10^{-4}	not appl.
7×10^{-4}	10	6×10^{-3}	0.05
7×10^{-3}	100	0.06	"
0.014	200	0.12	"
0.04	600	0.5	"
0.06	900	1	"
0.10	1500	5	"
0.13	1800	∞	"
0.2	1800	∞	0.043
0.5	"	"	0.032
1	"	"	0.025
5	"	"	0.015
10	"	"	0.012

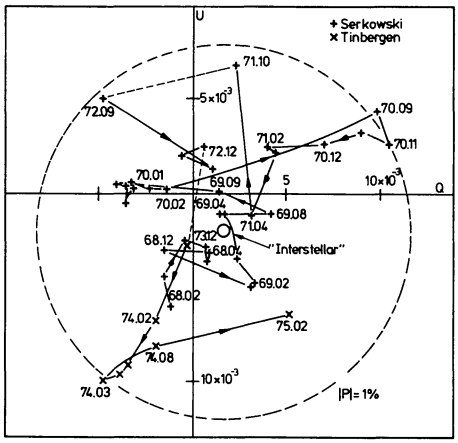

Fig. 6. Polarization vector at 430 nm (Serkowski) and 450 nm (Tinbergen), as it varied over the period 1968-1975. The observations suggest the occurrence of a single scattering element at any time, with a characteristic life time of the order of one year.

obtain (using k for n_e/n_H):

$$3 \approx P_{R15}/P_T = \frac{15 \times (0.1026)^4}{k} \cdot \left[1 + 1.4 \times 10^4 \cdot A \cdot (1+k) \left(\frac{a_d}{0.05}\right)^3\right]$$

$$\text{or: } 1.8 \times 10^3 k = 1 + x(1+k) \qquad (6)$$

$$\text{with } x = 1.4 \times 10^4 \cdot A \cdot \left(\frac{a_d}{0.05}\right)^3$$

We can now take $a_d = 0.05$ μm as an example and solve for A for each value of k we wish to assume. The choice of $a_d = 0.05$ μm is based on the core-mantle grain model. Since the short-wavelength deviations from the λ^{-4} law start at about $\lambda = 500$ nm, the condition for validity of Eq. (2a) also leads to about this value. The upper part of Table 4 lists the results.

Complete ionization ($k = \infty$) is incompatible with $A = 1$ and $a_d = 0.05$ μm. The lower part of Table 4 lists a few values of a_d for chosen A at $k = \infty$ ($A > 1$ would correspond to superabundance of silicon in the scattering cloud).

Eq. (6) is a relation between A, k and a_d. Another such relation might be obtained from theories of grain condensation (given that α Ori is an M2 Iab supergiant). Under equilibrium conditions, in a given stellar atmosphere high ionization implies a high temperature and hence a low condensed fraction, so that the function A(k) for a given assumed a_d will be monotonic decreasing. The observations define a similar function A'(k), which, however, is monotonic increasing (Table 4). A simultaneous solution for A and k should therefore be possible and one could then deduce limits on the radial distance of the scattering region. The reference to equilibrium conditions may sound farfetched for a turbulent element in a supergiant atmosphere,but the observational constraint is likely to remain a useful one when a more sophisticated treatment is applied to the problem. With the advent of efficient multichannel spectropolarimeters (e.g. McLean et al. 1979), a much more extensive investigation becomes feasible. One might for instance, look for differences in the time variations of the Thomson and Rayleigh contributions to the polarization.

b) Time variations

We may estimate a timescale for the scattering elements in α Ori in two ways. Judging from the direction of the p-vector, and from its length, it would seem that the polarizing configuration did not exist in December 1973, nor in February 1975, so that a life-time of approximately one year is indicated.

The polarization of α Ori has been measured quasi-continuously during the period 1968 through 1975. Figure 6 shows the polarization vector as measured by Serkowski (1971, 1977) at 430 nm, and by Tinbergen (this paper) at 450 nm. Although the first impression of the diagram is that of random motion around the 'interstellar' point, it is clear that there are periods, of the order of one year, during which remains roughly of the same strength and direction. This is in qualitative agreement with the detailed measurements of 1974. The time scale of about one year is of the same order as that of the random photospheric velocities (e.g. Goldberg 1979).

There is no evidence in our observations for variations of the ratio P_R/P_T with time scales less than 1 year.

The facts presented in this and the previous subsection point to an explanation of the polarization in terms of temporarily asymmetrically distributed scatterers or temporarily asymmetrically distributed photospheric light scattered by constant symmetrical cloud (Schwarzschild, 1975, p. 143). The observed timescale (of order one year) agrees with the predictions for a red supergiant (150-2000 days, as quoted by Schwarzschild (loc. cit., p. 142)).

c) Residuals at long wavelengths

While the observations in bands 3 to 6 (500-700 nm) can be very well described by Eq. 3 (and the short-wavelength deviations have a natural explanation in

terms of grain size, see Figs. 5 and 8), this is not the case for the longer wavelengths, neither for the direction, nor for the degree of polarization. We call $\underset{\sim}{p}_{calc}$ the p-value found from p_T and p_{R15} in Table 3 - which means basing the length of the vector on bands 3,4 and 5 - and taking as the direction of the vector the average of the directions for bands 3,4 and 5 (and sometimes 6). Then the residual vector is defined by $\underset{\sim}{p}_{res} = \underset{\sim}{p}_{intr} - \underset{\sim}{p}_{calc}$. In Fig. 7 this vector is given

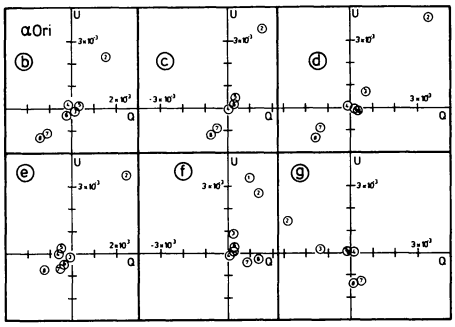

Fig. 7. Values of the 'residual polarization vector' $\underset{\sim}{p}_{res}$ for α Ori during the six observing periods b-g. The numbers 1-8 identify the passbands.

for α Ori for the several observational periods of Table 1. We refrain from giving the corresponding picture for α Sco; it has a roughly similar character. The residuals are not due to instrumental errors; they are much too large to have escaped notice during instrumental testing. They are also too large (by a factor 10 to 100) to be explained by the shell observed by McMillan & Tapia (1978).

Let us consider the observations in passband 8. The direction of $\underset{\sim}{p}_{res}$ (8) varies with time in a systematic way (Fig. 7). However, the scalar value, $|\underset{\sim}{p}_{res}|$ (8), hardly changes with time and is also independent of the variations of the general polarization (charactierized by $\underset{\sim}{p}$ (4)) and of the short-wavelength residuals (characterized by $\underset{\sim}{p}_{res}$ (2)), as shown in Fig. 9. We have not been able to find an explanation for the long-wavelength residuals.

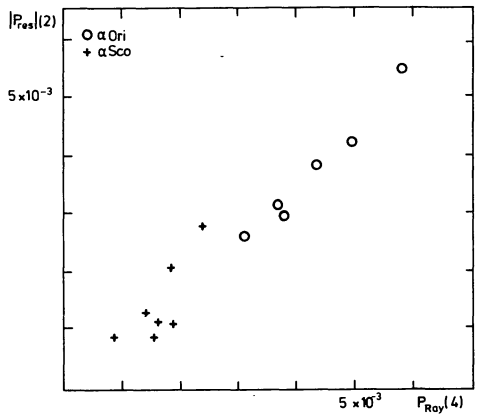

Fig. 8. A plot of p_{res} (2) against p_{Ray} (4) yields a fair linear relation, which suggests that the short-wavelength residuals are due to scattering at molecular or small dust species in the same scattering element responsible for the polarization in the medium passbands.

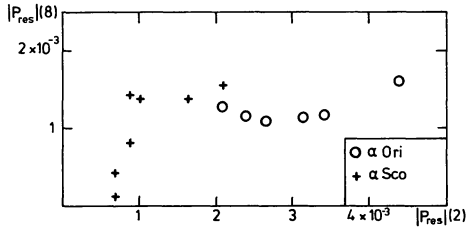

Fig. 9. p_{res} (8) against p_{res} (2)

5. CONCLUSION

The main component in the observed polarization of α Ori and α Sco follows a λ^{-4} law. The strength and direction of the polarization vary on a time scale of the order of one year. We conclude that there is evidence for polarization by atomic and dust scatterers, in a picture in general agreement with Schwarzschild's (1975). We have derived a relation between the amount of dust present and the degree of ionization in the scattering region. Other components in the measured polarization are a small interstellar or slowly varying circumstellar component (at least for α Ori) and residuals above 650 nm. We feel that a new programme, on more stars and carried out with a multi-channel spectropolarimeter, would be timely. It would necessarily extend over several years and it must obviously be coordinated with high-resolution spectroscopy such as that by Goldberg & Testerman (Goldberg 1979) and spatial interferometry of some kind.

ACKNOWLEDGEMENTS

Messrs. D. Hofstadt of ESO and D.F. Stevenson of the Leiden Southern Station put in considerable work to link the polarimeter to the respective data systems. Mr. J.J. Schafgans performed part of the reduction. These and other contributions are gratefully acknowledged.

Dr. K. Serkowski generously sent us his unpublished observations and allowed us to use them in this paper; they were used in constructing Figs 4 and 6. Prof. J.W. Hovenier, Prof. H.C. van de Hulst, Dr. K.A. van der Hucht, and Dr. J.R.W. Heintze made useful comments on the manuscript.

REFERENCES

Goldberg, L.: 1979, *Quarterly J. R.A.S.* 20, 361
Greenberg, J.M.: 1978, *'Cosmic Dust'*, Ed. J.A.M. McDonnell (Wiley Interscience)
McLean, I.S., Coyne, G.V., Frecker, J.E., Serkowski, K.: 1979, *Astrophys. J.* 228, 802
McMillan, R.S., Tapia, S.: 1978, *Astrophys. J.* 226, L87
Merrill, K.M.: 1977, in IAU Coll. 42 (Eds. R. Kippenhahn, J. Rahe, W. Strohmeier) Veröff. Remeis-Sternwarte Bamberg XI, no. 121, p. 462
Merrill, K.M., Stein, W.A.: 1976, *Publ. Astr. Soc. Pacific* 88, 285
Salpeter, E.E.: 1977, *Ann. Rev. Astron. and Astrophys.* 15, 267
Schwarzschild, M.: 1975, *Astrophys. J.* 195, 137
Serkowski, K.: 1971, *Kitt Peak Contribution* No. 554, p. 107
Serkowski, K.: 1977, private communication
Stothers, R., Leung, K.C.: 1971, *Astron. Astrophys.* 10, 290
Tinbergen, J.: 1973, *Astron. Astrophys.* 23, 25
Unsöld, A.: 1955, *Physik der Sternatmosphären*, 2nd. ed. (Springer, Berlin)